J|A|C|S
ARTICLES
Published on Web 05/22/2002

Recognition of Ten Base Pairs of DNA by Head-to-Head Hairpin Dimers

Philipp Weyermann and Peter B. Dervan*

Contribution from the Division of Chemistry and Chemical Engineering, California Institute of Technology, Pasadena, California 91125

Received February 19, 2002

Abstract: Hairpin polyamides coupled head-to head with alkyl linkers of varying lengths were synthesized, and their DNA binding properties were determined. The DNA binding affinities of six-ring hairpin dimers Im-Im-Py-(*R*)[Im-Im-Py-(*R*)$^{HNCO(CH)_nCO}\gamma$-Py-Py-Py-β-Dp]$^{NH}\gamma$-Im-Py-Py-β-Dp (**1**−**4**) (where $n = 1-4$) for their 10-bp, 11-bp, and 12-bp match sites 5′-TGGCATACCA-3′, 5′-TGGCATTACCA-3′, and 5′-TGGCATATACCA-3′ were determined by quantitative DNase I footprint titrations. The most selective dimer Im-Im-Py-(*R*)[Im-Im-Py-(*R*)$^{HNCO(CH_2)_2CO}\gamma$-Py-Py-Py-β-Dp]$^{NH}\gamma$-Im-Py-Py-β-Dp (**2**) binds the 10-bp site match site with an equilibrium association constant of $K_a = 7.5 \times 10^{10}$ M^{-1} and displays 25- and 140-fold selectivity over the 11-bp and 12-bp match sites, respectively. The affinity toward single base pair mismatched sequences is 4- to 8-fold lower if one hairpin module of the dimer is affected, but close to 200-fold lower if both hairpin modules face a single mismatch base pair. The head-to-head hairpin dimer motif expands the binding site size of DNA sequences targetable with polyamides.

Introduction

For the field of gene regulation by small molecules, the design of ligands for targeting DNA sites ≥10 bp in size remains an important goal.[1] Polyamides comprised of *N*-methylpyrrole (Py), *N*-methylimidazole (Im), and 3-hydroxypyrrole (Hp) amino acids are synthetic ligands that have an affinity and sequence specificity for DNA comparable to naturally occurring DNA binding proteins.[1a] DNA recognition depends on a code of side-by-side amino acid pairings usually oriented N- to C-terminus with respect to the 5′ to 3′ direction of the DNA helix in the minor groove.[1a] An Im/Py pair binds a G·C base pair, while a Py/Im pair recognizes C·G. A Py/Py pair is degenerate and recognizes either an A·T or a T·A base pair in preference to G·C and C·G. The discrimination of T·A from A·T by Hp/Py pairs completes the four base pair code. For targeting single sites in gigabase size DNA, it may be necessary to move beyond the eight-ring hairpins which target sites six base pairs in size. Studies of polyamide site size limitations suggest that beyond five consecutive rings, the ligand curvature fails to match the pitch of the DNA double helix, disrupting the hydrogen bonds and van der Waals interactions responsible for specific DNA recognition.[2] Replacement of Py with one or more flexible β-alanine amino acids can relieve these limitations and has allowed for design of ligands which target up to 16 bp of DNA.[3] An alternative approach to target large binding site sizes is to assemble modules of minor groove binding elements connected via optimized linkers without compromising DNA-binding affinity and sequence-specificity.[4] Six-ring hairpin polyamides[5] have been linked tail-to-turn with valeric acid (C_5) to provide head-to-tail dimers (tandem hairpins) which were shown to bind 10- and 11-bp target sites with high affinity and good selectivity.[6]

Hairpin modules linked turn-to-turn would provide head-to-head dimers and should be examined with the goal of targeting DNA binding sites of ≥10 bp (Figure 1). Two six-ring hairpins ImImPy-γ-PyPyPy-β-Dp (**5a**) and ImImPy-γ-ImPyPy-β-Dp (**6a**) were chosen which target different 5-bp sequences,[5] 5′-TGGTA-3′ and 5′-TGGCA-3′, respectively.[5] Hairpin dimers ImImPy-(*R*)[ImImPy-(*R*)$^{HNCO(CH)_nCO}\gamma$-PyPyPy-β-Dp]$^{NH}\gamma$-ImPyPy-β-Dp (**1**−**4**), where $n = 1-4$, were synthesized with an incrementally increasing alkyl linker (Figure 2) connecting the turns. The length of the linker chosen was based on results from model building to span two contiguous 5-bp sites, or 10-bp or 11-bp dimer binding sites. The six-ring hairpin polyamides ImImPy-(*R*)$^{H_2N}\gamma$-PyPyPy-β-Dp (**5b**) and ImImPy-(*R*)$^{H_2N}\gamma$-ImPyPy-β-Dp (**6b**) containing a primary amino group at the γ-turn were synthesized by solid-phase methods,[7] and coupled in

* To whom correspondence should be addressed. Phone: (626) 395 6002. Fax: (626) 683 8753. E-mail: dervan@caltech.edu.

(1) (a) Dervan, P. B. *Bioorg. Med. Chem.* **2001**, *9*, 2215. (b) Reddy, B. S.; Sharma, S. K.; Lown, J. W. *Curr. Med. Chem.* **2001**, *8*, 475. (c) Bailly, C.; Chaires, J. B. *Bioconjugate Chem.* **1998**, *9*, 513. (d) Chiang, S. Y.; Bruice, T. C.; Azizkhan, J. C.; Gawron, L.; Beerman, T. A. *Proc. Natl. Acad. Sci. U.S.A.* **1997**, *94*, 2811.

(2) (a) Kelly, J. J.; Baird, E. E.; Dervan, P. B. *Proc. Natl. Acad. Sci. U.S.A.* **1996**, *93*, 6981. (b) Kielkopf, C. L.; Baird, E. E.; Dervan, P. B.; Rees, D. C. *Nat. Struct. Biol.* **1998**, *5*, 104.

(3) (a) Trauger, J. W.; Baird, E. E.; Mrksich, M.; Dervan, P. B. *J. Am. Chem. Soc.* **1996**, *118*, 6160. (b) Swalley, S. E.; Baird, E. E.; Dervan, P. B. *Chem.-Eur. J.* **1997**, *3*, 1608. (c) Trauger, J. W.; Baird, E. E.; Dervan, P. B. *J. Am. Chem. Soc.* **1998**, *120*, 3534.

(4) (a) Dervan, P. B. *Science* **1986**, *232*, 464. (b) Satz, A. L.; Bruice, T. C. *J. Am. Chem. Soc.* **2001**, *123*, 2469.

(5) (a) Parks, M. E.; Baird, E. E.; Dervan, P. B. *J. Am. Chem. Soc.* **1996**, *118*, 6153. (b) Swalley, S. E.; Baird, E. E.; Dervan, P. B. *J. Am. Chem. Soc.* **1999**, *121*, 1113. (c) Herman, D. H.; Baird, E. E.; Dervan, P. B. *J. Am. Chem. Soc.* **1998**, *120*, 1382.

(6) (a) Herman, D. M.; Baird, E. E.; Dervan, P. B. *Chem.-Eur. J.* **1999**, *5*, 975. (b) Kers, I.; Dervan, P. B. *Bioorg. Med. Chem.*, in press.

10.1021/ja020258k CCC: $22.00

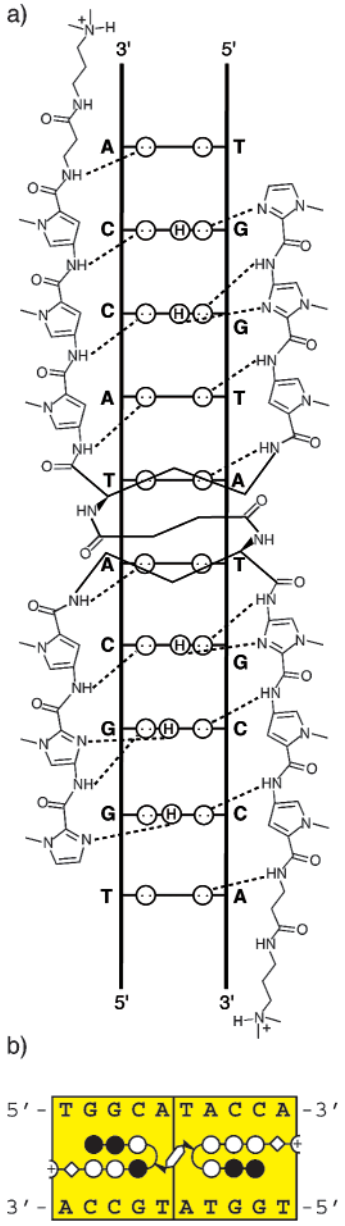

Figure 1. (a) Hydrogen-bonding model of the head-to-head hairpin dimer·DNA complex, ImImPy-(*R*)[ImImPy-(*R*)$^{HNCO(CH_2)_2CO}\gamma$-PyPyPy-β-Dp]$^{NH}\gamma$-ImPyPy-β-Dp and the 10-bp site 5′-TGGCATACCA-3′. Circles with two dots represent the lone pairs of N3 of purines and O2 of pyrimidines. Circles containing an H represent the N2 hydrogen of guanine. Putative hydrogen bonds are illustrated by dotted lines. (b) For a schematic binding model, Im and Py rings are represented as filled and open spheres, respectively. The β-residue and succinic acid linker are represented as an open diamond and a shaded hexagon, respectively. Individual 5-bp binding sites are shaded.

solution-phase chemistry to afford the 12-ring hairpin polyamide hetero-dimers **1**−**4**.

We report the DNA binding affinities of four hairpin dimers **1**−**4** for their 10-bp, 11-bp, and 12-bp match sites 5′-TGGCATACCA-3′, 5′-TGGCATTACCA-3′, and 5′-TGGCATATACCA-3′ (5-bp hairpin target sites are underlined), as well as the sequence selectivity of the most selective dimer **2** at its preferred 10-bp site over the 1-bp mismatch site 5′-TGGCAT**C**CCA-3′, and two individual 2-bp mismatch sites, 5′-TGG**G**AT**C**CCA-3′ and 5′-AGGTTT**C**C**G**T-3′ (mismatched base pairs are bold), respectively. Quantitative DNase I footprint titrations were employed to determine the equilibrium association constants (K_a) of the polyamides for DNA match and mismatch binding sites.[8] The precise binding site size was confirmed by MPE·Fe(II) footprinting, while affinity cleavage with **2**-EDTA·Fe determined the binding orientation of the hairpin dimer·DNA complex.[9]

Results

Synthesis. The two six-ring polyamides **5b** and **6b**[5] were prepared from Boc-β-PAM-resin by solid-phase synthesis[7a] (Figure 3). Hairpin polyamide **5b** was allowed to react with an alkyl diacid dihydroxysuccinimide ester $SuO_2C(CH_2)_nCO_2Su$ ($n = 1-4$)[11] to provide the modified six-ring hairpin polyamides ImImPy-(*R*)$^{HNCO(CH_2)_nCO_2H}\gamma$-PyPyPy-$\beta$-Dp (**5Ln**) ($n = 1-4$). The activated ester remaining on the diacid linker after reaction with the polyamide **5b** was hydrolyzed to the free acid under the conditions employed in the HPLC purification step. The purified **5Ln** ($n = 1-4$) was subsequently coupled in a second solution-phase step with six-ring hairpin polyamide **6b** using PyBop and HOBt to provide the 12-ring head-to-head linked hairpin dimers **1**−**4**. This combined solid-phase/solution-phase strategy allowed the preparation of the small library of dimers with different lengths of the alkyl linker connecting the individual six-ring hairpin modules **5b** and **6b**. The dimers **1**−**4** were characterized by ^{1}H NMR spectroscopy and MALDI-TOF mass spectrometry, as well as by analytical HPLC. An affinity cleaving analogue of **2**, conjugate **2-EDTA**, was synthesized by a slightly modified procedure which is described in the Supporting Information (Supporting Figure 1).

Optimum Binding Site Size. As a preliminary screen, quantitative DNase I footprint titrations[8] were performed to determine the optimum binding site size and whether any of the dimers **1**−**4** discriminate between 10-, 11-, and 12-bp match sites, 5′-TGGCATACCA-3′, 5′-TGGCATTACCA-3′, and 5′-TGGCATATACCA-3′ (Supporting Figure 2). Polyamide **1** preferentially binds the 10-bp site with high affinity ($K_a = 1.1 \times 10^{10}$ M^{-1}), but displays similar affinity toward the 11-bp site and the 12-bp site. Polyamide **2** binds the 10-bp site with higher affinity of $K_a = 5.4 \times 10^{10}$ M^{-1}, and, in addition, displays good selectivity versus the 11-bp site and 12-bp site (Table 1). Polyamides **3** and **4** reveal reduced affinity and poor discrimination between the 10-, 11-, and 12-bp sites (Table 1).

Specificity for Matched versus Mismatched Binding. In view of its favorable DNA-binding properties, dimer **2** with the C_4 linker was chosen for study of specificity toward mismatches within the optimum 10-bp binding site. In addition to the match site 5′-TGGCATACCA-3′, one 1-bp mismatch site, 5′-TGGCAT**C**CCA-3′, and two 2-bp mismatch sites, 5′-TGG**G**AT**C**CCA-3′ (site I) and 5′-AGGTTT**C**C**G**T-3′ (site II), were investigated by quantitative DNase I footprint titrations[8] (10 mM Tris-HCl, 10 mM KCl, 10 mM $MgCl_2$, and 5 mM $CaCl_2$, pH 7.0 and 22 °C, 48 h equilibration time) on a 5′-^{32}P-labeled 302-bp PCR amplified fragment from plasmid pPWLH1 (Figure 4)

(7) (a) Baird, E. E.; Dervan, P. B. *J. Am. Chem. Soc.* **1996**, *118*, 6141. (b) Wurtz, N. R.; Turner, J. M.; Baird, E. E.; Dervan, P. B. *Org. Lett.* **2001**, *3*, 1201.

(8) Trauger, J. W.; Dervan, P. B. *Methods Enzymol.* **2001**, *340*, 450.
(9) Brenowitz, M.; Senear, D. F.; Shea, M. A.; Ackers, G. K. *Methods Enzymol.* **1986**, *130*, 132.
(10) Hill, M.; Bechet, J.-J.; d'Albis, A. *FEBS Lett.* **1979**, *102*, 282.
(11) Sambrook, J.; Fritsch, E. F.; Maniatis, T. *Molecular Cloning*; Cold Spring Harbor Laboratory: Cold Spring Harbor, NY, 1989.

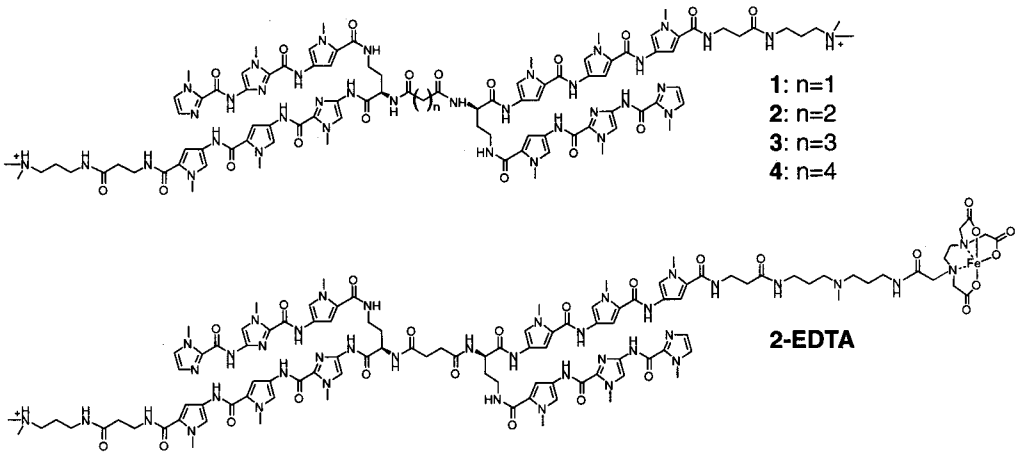

Figure 2. (a) Structures of the head-to-head hairpin dimers **1**−**4**, as well as affinity cleavage conjugate **2-EDTA**.

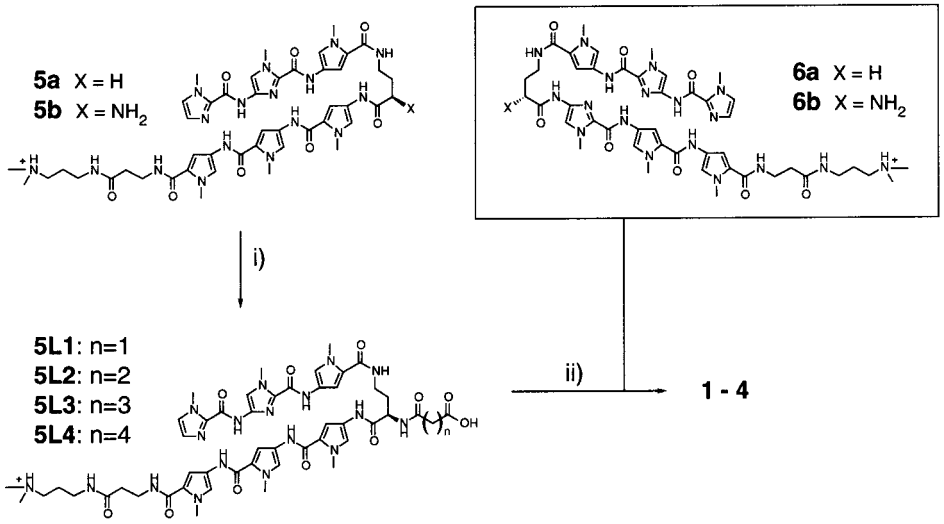

Figure 3. Synthesis of the head-to-head linked hetero dimers **1**−**4** from two different six-ring hairpin polyamides **5b** and **6b**: (i) $SuO_2C(CH_2)_nCO_2Su$ (where $n = 1-4$), DIEA, DMSO/DMF 1:1, 2 h; (ii) PyBop, HOBt, DIEA, DMF, 4 h.

to determine the equilibrium association constants. Whereas the first three sites (match site, 1-bp mismatch site, and 2-bp mismatch site I) were designed into the plasmid, the fourth site, 2-bp mismatch site II, was inherently present on the parent plasmid pUC19, used for the construction of pPWLH1. For that reason, it differs from the other three binding sites in sequence and has opposite orientation as well. Under the conditions mentioned above, polyamide **2** binds its 10-bp match site with an equilibrium association constant of $K_a = 7.5 \times 10^{10}$ M^{-1}. The 1-bp mismatch site is bound with $K_a = 2.0 \times 10^{10}$ M^{-1}, which corresponds to a roughly 4-fold specificity. The two 2-bp mismatch sites show remarkably different behavior; whereas the 2-bp mismatch site II, with the two mismatched base pairs inside the same individual six-ring hairpin polyamide half of the dimer, is bound with an affinity of $K_a = 1 \times 10^{10}$ M^{-1}, the 2-bp mismatch site II, where the two mismatched base pairs are distributed over both six-ring hairpin polyamide halves of the dimer, is only bound with an affinity of $K_a = 4.0 \times 10^8$ M^{-1}. This corresponds to a specificity of roughly 8-fold toward 2-bp mismatch site II, but almost 200-fold over 2-bp mismatch site I (Table 2).

Binding Orientation. MPE·Fe(II) footprinting[8] (20 mM HEPES, 200 mM NaCl, pH 7.0 and 22 °C, 18 h equilibration time) on the same restriction fragment revealed that the size of the cleavage protection patterns for bound polyamide **2** at all four binding sites on the DNA fragments is 10 bp in size and consistent with both hairpins bound in the minor groove of DNA. Affinity cleavage experiments[9] (20 mM HEPES, 200 mM NaCl, pH 7.0 and 22 °C, 18 h equilibration time) with **2-EDTA**·Fe, which has an EDTA appended to one unique tail (of module **5**), were used as a control to confirm the polyamide binding orientation. Cleavage of DNA by **2-EDTA**·Fe reveals strong cleavage patterns proximal to the 3′ side of the 10-bp match site 5′-TGGCATACCA-3′, the 1-bp mismatch site 5′-TGGCAT**C**CCA-3′, and the 2-bp mismatch site I 5′-TGG**G**AT**C**CCA-3′, as well as proximal to the 5′ side of the 2-bp mismatch site II 5′-AGGTTT**CC**G**T**-3′, consistent with the formation of a major orientation preference for each hairpin-dimer·DNA complex at all four sites. Minor cleavage is observed at the opposite side of the first two binding sites, 5′-TGGCATACCA-3′ and 5′-TGGCAT**C**CCA-3′, indicating that some degree of reverse orientation binding is possible. The reverse orientation corresponds to one additional mismatch as compared to the forward orientation in these two cases. The 2-bp mismatch site I is palindromic and consequently shows strong cleavage patterns both on the 3′ side and on the 5′ side, whereas the 2-bp mismatch site II does not show any indication of reverse orientation binding. Reverse orientation binding in this case

Table 1. Equilibrium Association Constants K_a [M^{-1}] of Hairpin Dimers **1**−**4** and of Parent Six-Ring Hairpin Polyamides **5a** and **6a**[a,b]

Polyamide	10-bp Binding Site	11-bp Binding Site	12-bp Binding Site
		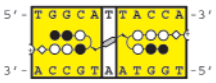	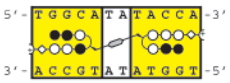
5a [5a] **6a** [5b]	[c] [d]	$1.0 \cdot 10^8$ (± 0.1) [c] $5.0 \cdot 10^7$ (± 0.3) [d]	[c] [d]
1	$1.1 \cdot 10^{10}$ (± 0.5)	$4.1 \cdot 10^9$ (± 0.9) *2.6* [e]	$2.1 \cdot 10^9$ (± 1.0) *5.2* [f]
2	$5.4 \cdot 10^{10}$ (± 1.1)	$2.2 \cdot 10^9$ (± 0.6) *25* [e]	$3.7 \cdot 10^8$ (± 1.4) *146* [f]
3	$1.5 \cdot 10^{10}$ (± 0.2)	$7.0 \cdot 10^9$ (± 1.2) *2.1* [e]	$3.2 \cdot 10^9$ (± 0.5) *4.7* [f]
4	$5.0 \cdot 10^9$ (± 1.8)	$3.5 \cdot 10^9$ (± 2.0) *1.4* [e]	$3.5 \cdot 10^8$ (± 0.2) *14* [f]

[a] The reported association constants K_a are the average values obtained from three DNase I footprint titration experiments. [b] The assays were carried out at 22 °C at pH 7.0 in the presence of 10 mM Tris-HCl, 10 mM KCl, 10 mM $MgCl_2$, and 5 mM $CaCl_2$ with an equilibration time of 36 h. The 10-bp, 11-bp, and 12-bp match binding sites are indicated with a schematic illustration of the binding mode. [c] The association constant K_a of **5a** for its 5′-TGGTA-3′ 5-bp match site was determined[5a] on a different plasmid, but it is expected to be very similar on the three binding sites indicated above. [d] The association constant K_a of **6a** for its 5′-TGGCA-3′ 5-bp match site was determined[5b] on a different plasmid, but it is expected to be very similar on the three binding sites indicated above. [e] Specificity of 10-bp versus 11-bp match site calculated as K_a(10-bp site)/K_a(11-bp site). [f] Specificity of 10-bp versus 12-bp match site calculated as K_a(10-bp site)/K_a(12-bp site).

Table 2. Equilibrium Association Constants K_a [M^{-1}] and Specificity of Hairpin Polyamide Dimer **2**[a,b]

Binding Site		K_a [M^{-1}]	Specificity
Match Site		$7.5 \cdot 10^{10}$ (± 0.9)	
1-bp Mismatch Site		$2.0 \cdot 10^{10}$ (± 0.5)	3.8 [c]
2-bp Mismatch Site I		$4.0 \cdot 10^8$ (± 3.8)	187 [d]
2-bp Mismatch Site II		$1.0 \cdot 10^{10}$ (± 0.0)	7.5 [e]

[a] The reported association constants K_a are the average values obtained from three DNase I footprint titration experiments. [b] The assays were carried out at 22 °C at pH 7.0 in the presence of 10 mM Tris-HCl, 10 mM KCl, 10 mM $MgCl_2$, and 5 mM $CaCl_2$ with an equilibration time of 48 h. The match, 1-bp mismatch, and 2-bp mismatch binding sites are indicated with a schematic illustration of the binding mode. [c] Specificity of match site versus 1-bp mismatch site calculated as K_a(match site)/K_a(1-bp mismatch site). [d] Specificity of match site versus 2-bp mismatch site I calculated as K_a(match site)/K_a(2-bp mismatch site I). [e] Specificity of match site versus 2-bp mismatch site II calculated as K_a(match site)/K_a(2-bp mismatch site II).

would result in two mismatched base pairs for each six-ring hairpin polyamide partner of the dimer and can be expected to be unfavorable.

Discussion

In the series of head-to-head hairpin dimers, polyamide **2** with the C_4 linker has the most favorable DNA-binding properties with regard to specificity and affinity. It binds a 10-bp site with 25-fold and 140-fold preference over 11-bp and 12-bp sites, respectively. None of the dimers **1**−**4** target sequences longer than 10 bp with decent selectivity. The poor binding at the 12-bp site suggests that the C_3−C_6 linker lengths are insufficient to span this site which is supported by model building. However, model building also suggests that dimers **3** and **4** should have a sufficiently long linker to span the 11-bp site. Yet the binding affinity data fail to reveal any preference for this site versus the shorter 10-bp site. This finding is most likely due to the flexibility of the linker domain and suggests that for specific 11-bp binders, rigid linkers may need to be examined.

The head-to-head dimer displays improved affinities by several orders of magnitude over the parent six-ring hairpin modules. This parallels our earlier findings in the head-to-tail tandem hairpin series.[6] However, the specificity toward mismatched sequences is modest if only one six-ring hairpin module of the dimer is affected. Good specificity is retained only if *both* six-ring hairpin modules in the dimer face a mismatched base pair. The linker is flexible, and both hairpins prefer contact to the hydrophobic DNA minor groove, even if one module is

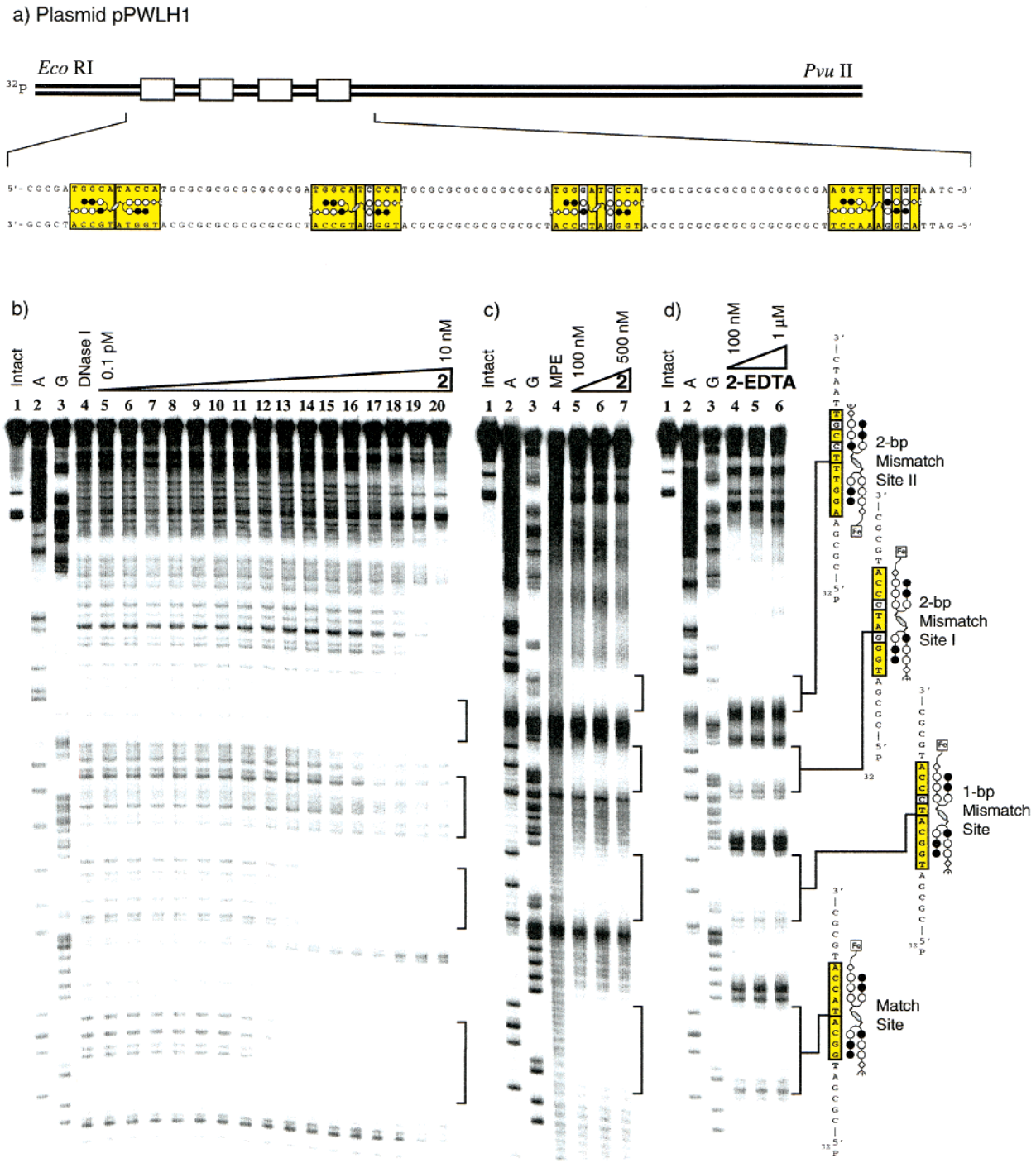

Figure 4. (a) Illustration of the *Eco*RI/*Pvu*II restriction fragment derived from plasmid pPWLH1, containing 10-bp match, single mismatch, and double mismatch target sites. Im and Py rings are represented as filled and open spheres, respectively. The β-residue and diacid linker are represented as an open diamond and a shaded hexagon, respectively. Individual 5-bp binding sites are shaded; mismatch positions are boxed. (b) Footprinting experiments with dimer (**2**) on the 5′-^{32}P-labeled 302-bp PCR amplified DNA fragment derived from the plasmid pPWLH1. Quantitative DNase I footprint titration experiment with **2**: lane 1, intact DNA; lane 2, A-specific reaction; lane 3, G-specific reaction; lane 4, DNase I standard; lanes 5−20, 0.1 pM, 0.2 pM, 0.5 pM, 1 pM, 2 pM, 5 pM, 10 pM, 20 pM, 50 pM, 100 pM, 200 pM, 500 pM, 1 nM, 2 nM, 5 nM, 10 nM **2**. All reactions contained 10 kcpm labeled DNA and were carried out at 22 °C at pH 7.0 in the presence of 10 mM Tris-HCl, 10 mM KCl, 10 mM $MgCl_2$, and 5 mM $CaCl_2$ with an equilibration time of 48 h. (c) MPE·Fe(II) footprint titration experiment with **2**: lane 1, intact DNA; lane 2, A-specific reaction; lane 3, G-specific reaction; lane 4, MPE·Fe(II) standard; lanes 5−7, 100 nM, 200 nM, 500 nM **2**. All reactions contained 20 kcpm 5′-labeled DNA and were carried out at 22 °C at pH 7.0 in the presence of 20 mM HEPES and 200 mM NaCl with an equilibration time of 18 h. (d) Affinity cleaving titration experiment with **2-EDTA**: lane 1, intact DNA; lane 2, A-specific reaction; lane 3, G-specific reaction; lanes 4−6, 100 nM, 500 nM, 1 μM **2-EDTA**. All reactions contained 20 kcpm 5′-labeled DNA and were carried out at 22 °C at pH 7.0 in the presence of 20 mM HEPES and 200 mM NaCl with an equilibration time of 18 h. The four sites 5′-TGGCATACCA-3′ (match site), 5′-TGGCAT**C**CCA-3′ (single mismatch site), 5′-TGG**G**AT**C**CCA-3′ (double mismach site I), and 5′-AGGTTT**C**C**G**T-3′ (double mismatch site II) that were analyzed are shown on the right side of the gel.

bound mismatched. Apparently, nonspecific minor groove binding adds a significant amount of free energy to the binding event once one hairpin in the dimer has bound to its match site in optimal geometry for specific hydrogen bond contacts with

the floor of the minor groove. It remains to be seen in further studies whether rigid linkers of the same length can provide better specificity toward these types of mismatches due to an increased preorganization of both modules and a tighter cooperative fit requirement for the target DNA structure, thus forcing more unfavorable interactions to occur upon mismatched binding of either module.

Experimental Section

Im-Im-Py-(*R*)$^{H_2N}\gamma$-Py-Py-Py-β-Dp (5b). Im-Im-Py-(*R*)$^{HNFmoc}\gamma$-Py-Py-Py-β-PAM-resin was synthesized in a stepwise fashion by manual solid-phase synthesis methods[7a] from Boc-β-PAM-resin (0.87 mmol/g). A sample of Im-Im-Py-(*R*)$^{HNFmoc}\gamma$-Py-Py-Py-β-PAM-resin (300 mg) was placed in a glass 20 mL peptide synthesis vessel and treated with neat *N*,*N*′-(dimethylamino)propylamine (2 mL) at 55 °C with periodic agitation for 18 h. The reaction mixture was filtered to remove resin; then 0.1% (wt/v) TFA was added (6 mL), and the resulting solution was purified by reversed phase HPLC. Im-Im-Py-(*R*)$^{H_2N}\gamma$-Py-Py-Py-β-Dp (**5b**) was recovered upon lyophilization of the appropriate fractions as a white powder (32.6 mg, 23% recovery). UV (H_2O): λ_{max} 260 (28 000), 310 (52 140). ^{1}H NMR (DMSO-d_6): δ 10.57 (s, 1H), 10.36 (s, 1H), 9.99 (s, 1H), 9.90 (s, 1H), 9.72 (s, 1H), 9.29 (bs, 1H), 8.24−8.34 (bm, 3H), 7.92−8.18 (m, 2H), 7.58 (s, 1H), 7.47 (d, 1H, J = 0.9 Hz), 7.26 (s, 1H), 7.23 (d, 1H, J = 1.8 Hz), 7.15 (d, 1H, J = 1.8 Hz), 7.08 (d, 1H, J = 0.9 Hz), 7.06 (s, 1H), 7.05 (s, 1H), 6.94 (d, 1H, J = 1.8 Hz), 6.89 (d, 1H, J = 1.8 Hz), 4.01 (s, 3H), 4.00 (s, 3H), 3.96−4.02 (m, 1H), 3.87 (s, 3H), 3.84 (s, 3H), 3.83 (s, 3H), 3.80 (s, 3H), 3.22−3.44 (m, 4H), 3.06−3.16 (m, 2H), 2.96−3.06 (m, 2H), 2.75 (d, 6H, J = 4.8 Hz), 2.35 (t, 2H, J = 7.2 Hz), 1.92−2.04 (m, 2H), 1.68−1.80 (m, 2H). MALDI-TOF-MS calcd. for $C_{46}H_{61}N_{18}O_8$ (M + H): 993.5. Found: 993.6.

Im-Im-Py-(*R*)$^{H_2N}\gamma$-Im-Py-Py-β-Dp (6b). Im-Im-Py-(*R*)$^{HNFmoc}\gamma$-Im-Py-Py-β-PAM-resin was synthesized in a stepwise fashion by manual solid-phase synthesis methods[7a] from Boc-β-PAM-resin (0.87 mmol/g). A sample of Im-Im-Py-(*R*)$^{HNFmoc}\gamma$-Im-Py-Py-β-PAM-resin (300 mg) was placed in a glass 20 mL peptide synthesis vessel and treated with neat *N*,*N*′-(dimethylamino)propylamine (2 mL) at 55 °C with periodic agitation for 18 h. The reaction mixture was filtered to remove resin; then 0.1% (wt/v) TFA was added (6 mL), and the resulting solution was purified by reversed phase HPLC. Im-Im-Py-(*R*)$^{H_2N}\gamma$-Im-Py-Py-β-Dp (**6b**) was recovered upon lyophilization of the appropriate fractions as a white powder (22.7 mg, 16% recovery). UV (H_2O): λ_{max} 260 (20 800), 310 (52 140). ^{1}H NMR (DMSO-d_6): δ 11.02 (s, 1H), 10.36 (s, 1H), 10.11 (s, 1H), 9.92 (s, 1H), 9.73 (s, 1H), 9.35 (bs, 1H), 8.84 (bs, 2H), 8.21 (t, 1H, J = 5.5 Hz), 7.97−8.10 (m, 2H), 7.58 (s, 1H), 7.54 (s, 1H), 7.47 (d, 1H, J = 0.9 Hz), 7.26 (d, 1H, J = 1.8 Hz), 7.25 (d, 1H, J = 1.8 Hz), 7.15 (s, 2H), 7.08 (d, 1H, J = 0.9 Hz), 7.04 (d, 1H, J = 1.8 Hz), 6.88 (d, 1H, J = 1.8 Hz), 4.01 (s, 3H), 4.00 (s, 3H), 3.98 (s, 3H), 3.93−3.97 (m, 1H), 3.85 (s, 3H), 3.81 (s, 3H), 3.80 (s, 3H), 3.25−3.43 (m, 4H), 3.06−3.16 (m, 2H), 2.96−3.06 (m, 2H), 2.75 (d, 6H, J = 4.8 Hz), 2.35 (t, 2H, J = 7.2 Hz), 1.94−2.05 (m, 2H), 1.68−1.80 (m, 2H). MALDI-TOF-MS calcd. for $C_{45}H_{60}N_{19}O_8$ (M + H): 994.5. Found: 994.6.

General Procedure for the Attachment of the Linker. Im-Im-Py-(*R*)$^{H_2N}\gamma$-Py-Py-Py-β-Dp (**5b**) (5.0 mmol, 5.0 mg) was dissolved in 200 mL of dry DMF. A solution of the appropriate diacid dihydroxysuccinimide ester $SuO_2C(CH_2)_nCO_2Su$ (50.0 mmol, 10.0 equiv; where n = 1, 2, 3, or 4) in 200 mL of dry DMSO was added, followed by DIEA (200 mL). The reaction mixture was shaken at room temperature for 2 h; then 0.1% (wt/v) TFA was added (6 mL), and the resulting solution was purified by reversed phase HPLC. The coupling products Im-Im-Py-(*R*)$^{HNCO(CH_2)_nCO_2H}\gamma$-Py-Py-Py-$\beta$-Dp (**5Ln**) (where n = 1−4) were recovered upon lyophilization of the appropriate fractions.

Im-Im-Py-(*R*)$^{HNCOCH_2CO_2H}\gamma$-Py-Py-Py-β-Dp (5L1). This was obtained using the activated diester of malonic acid, $SuO_2CCH_2CO_2Su$. Off-white powder (4.2 mg, 78% isolated yield). UV (H_2O): λ_{max} 260 (28 000), 310 (52 140). ^{1}H NMR (DMSO-d_6): δ 10.31 (s, 1H), 10.02 (s, 1H), 9.95 (s, 1H), 9.90 (s, 1H), 9.73 (s, 1H), 9.22 (bs, 1H), 8.50 (d, 1H, J = 8.1 Hz), 8.02−8.09 (m, 2H), 8.00 (t, 1H, J = 5.4 Hz), 7.56 (s, 1H), 7.46 (d, 1H, J = 0.8 Hz), 7.23 (d, 1H, J = 1.6 Hz), 7.22 (d, 1H, J = 1.6 Hz), 7.18 (d, 1H, J = 1.6 Hz), 7.17 (d, 1H, J = 1.6 Hz), 7.08 (d, 1H, J = 0.8 Hz), 7.04 (d, 1H, J = 1.6 Hz), 6.97 (d, 1H, J = 1.6 Hz), 6.92 (d, 1H, J = 1.6 Hz), 6.87 (d, 1H, J = 1.6 Hz), 4.45 (q, 1H, J = 7.2 Hz), 4.00 (s, 3H), 3.99 (s, 3H), 3.83 (s, 6H), 3.79 (s, 6H), 3.32−3.41 (m, 2H), 3.27 (s, 2H), 3.05−3.21 (m, 4H), 2.84−3.05 (m, 2H), 2.74 (d, 6H, J = 4.8 Hz), 2.35 (t, 2H, J = 7.2 Hz), 1.67−2.03 (m, 4H). MALDI-TOF-MS calcd. for $C_{49}H_{63}N_{18}O_{11}$ (M + H): 1079.5. Found: 1079.5.

Im-Im-Py-(*R*)$^{HNCO(CH_2)_2CO_2H}\gamma$-Py-Py-Py-$\beta$-Dp (5L2). This was obtained using the activated diester of succinic acid, $SuO_2C(CH_2)_2CO_2Su$. White powder (4.4 mg, 71% isolated yield). UV (H_2O): λ_{max} 260 (28 000), 310 (52 140). ^{1}H NMR (DMSO-d_6): δ 10.29 (s, 1H), 9.95 (s, 1H), 9.92 (s, 1H), 9.89 (s, 1H), 9.73 (s, 1H), 9.22 (bs, 1H), 8.25 (d, 1H, J = 8.1 Hz), 7.99−8.09 (m, 2H), 7.98 (t, 1H, J = 5.4 Hz), 7.57 (s, 1H), 7.46 (d, 1H, J = 0.8 Hz), 7.22 (d, 1H, J = 1.6 Hz), 7.21 (d, 1H, J = 1.6 Hz), 7.18 (d, 1H, J = 1.6 Hz), 7.16 (d, 1H, J = 1.6 Hz), 7.07 (d, 1H, J = 0.8 Hz), 7.04 (d, 1H, J = 1.6 Hz), 6.98 (d, 1H, J = 1.6 Hz), 6.93 (d, 1H, J = 1.6 Hz), 6.87 (d, 1H, J = 1.6 Hz), 4.41 (q, 1H, J = 7.2 Hz), 4.00 (s, 6H), 3.83 (s, 6H), 3.80 (s, 6H), 3.32−3.43 (m, 2H), 3.05−3.32 (m, 4H), 2.94−3.05 (m, 2H), 2.76−2.85 (m, 2H), 2.74 (d, 6H, J = 4.8 Hz), 2.40−2.47 (m, 2H), 2.34 (t, 2H, J = 7.2 Hz), 1.66−2.04 (m, 4H). MALDI-TOF-MS calcd. for $C_{50}H_{65}N_{18}O_{11}$ (M + H): 1093.5. Found: 1093.6.

Im-Im-Py-(*R*)$^{HNCO(CH_2)_3CO_2H}\gamma$-Py-Py-Py-$\beta$-Dp (5L3). This was obtained using the activated diester of glutaric acid, $SuO_2C(CH_2)_3CO_2Su$. White powder (4.2 mg, 78% isolated yield). UV (H_2O): λ_{max} 260 (20 800), 310 (52 140). ^{1}H NMR (DMSO-d_6): δ 10.31 (s, 1H), 10.05 (s, 1H), 9.94 (s, 1H), 9.90 (s, 1H), 9.73 (s, 1H), 9.29 (bs, 1H), 8.18 (d, 1H, J = 8.1 Hz), 8.02−8.10 (m, 2H), 8.01 (t, 1H, J = 5.4 Hz), 7.57 (s, 1H), 7.46 (d, 1H, J = 0.8 Hz), 7.23 (d, 1H, J = 1.6 Hz), 7.22 (d, 1H, J = 1.6 Hz), 7.19 (d, 1H, J = 1.6 Hz), 7.16 (d, 1H, J = 1.6 Hz), 7.07 (d, 1H, J = 0.8 Hz), 7.04 (d, 1H, J = 1.6 Hz), 6.98 (d, 1H, J = 1.6 Hz), 6.92 (d, 1H, J = 1.6 Hz), 6.87 (d, 1H, J = 1.6 Hz), 4.41 (q, 1H, J = 7.2 Hz), 4.00 (s, 3H), 3.99 (s, 3H), 3.84 (s, 6H), 3.80 (s, 6H), 3.33−3.43 (m, 2H), 3.05−3.28 (m, 4H), 2.94−3.05 (m, 2H), 2.74 (d, 6H, J = 4.8 Hz), 2.34 (t, 2H, J = 7.2 Hz), 2.16−2.28 (m, 4H), 1.66−1.99 (m, 6H). MALDI-TOF-MS calcd. for $C_{51}H_{67}N_{18}O_{11}$ (M + H): 1107.5. Found: 1107.6.

Im-Im-Py-(*R*)$^{HNCO(CH_2)_4CO_2H}\gamma$-Py-Py-Py-$\beta$-Dp (5L4). This was obtained using the activated diester of adipic acid, $SuO_2C(CH_2)_4CO_2Su$. Yellow powder (3.6 mg, 65% isolated yield). UV (H_2O): λ_{max} 260 (28 000), 310 (52 140). ^{1}H NMR (DMSO-d_6): δ 10.30 (s, 1H), 10.05 (s, 1H), 9.93 (s, 1H), 9.89 (s, 1H), 9.71 (s, 1H), 9.17 (bs, 1H), 8.15 (d, 1H, J = 8.1 Hz), 7.96−8.10 (m, 3H), 7.56 (s, 1H), 7.45 (d, 1H, J = 0.8 Hz), 7.22 (d, 1H, J = 1.6 Hz), 7.21 (d, 1H, J = 1.6 Hz), 7.18 (d, 1H, J = 1.6 Hz), 7.15 (d, 1H, J = 1.6 Hz), 7.06 (d, 1H, J = 0.8 Hz), 7.04 (d, 1H, J = 1.6 Hz), 6.98 (d, 1H, J = 1.6 Hz), 6.91 (d, 1H, J = 1.6 Hz), 6.86 (d, 1H, J = 1.6 Hz), 4.40 (q, 1H, J = 7.2 Hz), 3.99 (s, 3H), 3.98 (s, 3H), 3.83 (s, 6H), 3.79 (s, 6H), 3.04−3.43 (m, 6H), 2.94−3.04 (m, 2H), 2.73 (d, 6H, J = 4.8 Hz), 2.33 (t, 2H, J = 7.2 Hz), 2.11−2.25 (m, 2H), 1.86−2.04 (m, 2H), 1.62−1.80 (m, 2H), 1.38−1.60 (m, 6H). MALDI-TOF-MS calcd. for $C_{52}H_{69}N_{18}O_{11}$ (M + H): 1121.5. Found: 1121.7.

General Procedure for the Coupling with the Second Hairpin Polyamide. To a solution of Im-Im-Py-(*R*)$^{HNCO(CH_2)_nCO_2H}\gamma$-Py-Py-Py-$\beta$-Dp (**5Ln**) (where n = 1−4) (2.0 μmol) and Im-Im-Py-(*R*)$^{H_2N}\gamma$-Im-Py-Py-β-Dp (**6b**) (2.0 μmol, 2.0 mg) in 200 μL of dry DMF was added HOBt (20.0 μmol, 4.3 mg, 10.0 equiv) followed by PyBop (10.0 μmol, 7.3 mg, 5.0 equiv) and DIEA (100 μL). The reaction mixture was shaken at room temperature for 4 h; then 0.1% (wt/v) TFA was added (6 mL), and the resulting solution was purified by reversed phase HPLC.

The head-to-head linked hairpin polyamide dimers **1**−**4** were recovered upon lyophilization of the appropriate fractions.

Im-Im-Py-(*R*)[Im-Im-Py-(*R*)^{HNCOCH_2CO}*γ*-Py-Py-Py-*β*-Dp]^{NH}*γ*-Im-Py-Py-*β*-Dp (1). This was obtained from Im-Im-Py-(*R*)^{HNCOCH_2CO_2H}*γ*-Py-Py-Py-*β*-Dp (**5L1**) as a white powder (0.3 mg, 7% isolated yield). UV (H_2O): λ_{max} 260 (56 000), 310 (104 280). ^{1}H NMR (DMSO-d_6): δ 10.43 (s, 1H), 10.28 (s, 1H), 10.27 (s, 1H), 10.15 (s, 1H), 10.08 (s, 1H), 9.92 (s, 1H), 9.90 (s, 1H), 9.88 (s, 1H), 9.70 (s, 2H), 9.42 (bs, 2H), 8.37 (d, 1H, J = 7.6 Hz), 8.27 (d, 1H, J = 7.6 Hz), 7.97−8.04 (m, 6H), 7.55 (s, 2H), 7.46 (s, 1H), 7.45 (s, 2H), 7.24 (d, 1H, J = 1.5 Hz), 7.23 (d, 2H, J = 1.5 Hz), 7.21 (s, 2H), 7.15 (s, 1H), 7.14 (d, 1H, J = 1.5 Hz), 7.13 (d, 1H, J = 1.5 Hz), 7.06 (d, 1H, J = 1.5 Hz), 7.05 (d, 1H, J = 1.5 Hz), 7.04 (s, 2H), 6.99 (d, 1H, J = 1.5 Hz), 6.98 (s, 2H), 6.87 (s, 2H), 4.61 (q, 1H, J = 6.8 Hz), 4.47 (q, 1H, J = 6.8 Hz), 4.00 (s, 6H), 3.99 (s, 6H), 3.94 (s, 3H), 3.84 (s, 3H), 3.83 (s, 3H), 3.80 (s, 12H), 3.79 (s, 3H), 3.08−3.18 (m, 8H), 2.98−3.07 (m, 8H), 2.76 (s, 2H), 2.74 (d, 12H, J = 5.0 Hz), 2.31−2.39 (m, 4H), 1.70−1.82 (m, 2H), 1.49−1.70 (m, 4H), 1.40−1.49 (m, 2H). MALDI-TOF-MS calcd. for $C_{94}H_{120}N_{37}O_{18}$ (M + H): 2055.0. Found: 2055.1.

Im-Im-Py-(*R*)[Im-Im-Py-(*R*)$^{HNCO(CH_2)_2CO}$*γ*-Py-Py-Py-*β*-Dp]^{NH}*γ*-Im-Py-Py-*β*-Dp (2). This was obtained from Im-Im-Py-(*R*)$^{HNCO(CH_2)_2CO_2H}$*γ*-Py-Py-Py-*β*-Dp (**5L2**) as a white powder (0.7 mg, 18% isolated yield). UV (H_2O): λ_{max} 260 (56 000), 310 (104 280). ^{1}H NMR (DMSO-d_6): δ 10.28 (s, 2H), 10.27 (s, 1H), 10.10 (s, 1H), 9.98 (s, 1H), 9.92 (s, 1H), 9.89 (s, 1H), 9.88 (s, 1H), 9.70 (s, 2H), 9.22 (bs, 2H), 8.26 (d, 1H, J = 7.6 Hz), 8.21 (d, 1H, J = 7.6 Hz), 7.96−8.06 (m, 6H), 7.56 (s, 2H), 7.45 (s, 3H), 7.22 (d, 1H, J = 1.5 Hz), 7.17−7.21 (m, 4H), 7.15 (s, 2H), 7.09 (s, 1H), 7.06 (s, 2H), 6.99 (s, 3H), 6.96 (d, 1H, J = 1.5 Hz), 6.88 (d, 2H, J = 1.5 Hz), 4.54 (q, 1H, J = 6.8 Hz), 4.43 (q, 1H, J = 6.8 Hz), 4.00 (s, 6H), 3.99 (s, 6H), 3.95 (s, 3H), 3.84 (s, 3H), 3.83 (s, 3H), 3.82 (s, 3H), 3.80 (s, 9H), 3.79 (s, 3H), 3.05−3.20 (m, 8H), 2.95−3.05 (m, 8H), 2.74 (d, 12H, J = 5.0 Hz), 2.42−2.49 (m, 4H), 2.32−2.39 (m, 4H), 1.70−1.79 (m, 2H), 1.60−1.68 (m, 2H), 1.52−1.59 (m, 2H), 1.41−1.51 (m, 2H). MALDI-TOF-MS calcd. for $C_{95}H_{122}N_{37}O_{18}$ (M + H): 2069.0. Found: 2069.1.

Im-Im-Py-(*R*)[Im-Im-Py-(*R*)$^{HNCO(CH_2)_3CO}$*γ*-Py-Py-Py-*β*-Dp]^{NH}*γ*-Im-Py-Py-*β*-Dp (3). This was obtained from Im-Im-Py-(*R*)$^{HNCO(CH_2)_3CO_2H}$*γ*-Py-Py-Py-*β*-Dp (**5L3**) as a white powder (0.8 mg, 18% isolated yield). UV (H_2O): λ_{max} 260 (56 000), 310 (104 280). ^{1}H NMR (DMSO-d_6): δ 10.42 (s, 1H), 10.29 (s, 1H), 10.28 (s, 1H), 10.15 (s, 1H), 10.10 (s, 1H), 9.93 (s, 1H), 9.89 (s, 1H), 9.88 (s, 1H), 9.70 (s, 2H), 9.21 (bs, 2H), 8.34 (d, 1H, J = 7.6 Hz), 8.29 (d, 1H, J = 7.6 Hz), 7.96−8.08 (m, 6H), 7.56 (s, 2H), 7.47 (s, 1H), 7.45 (s, 2H), 7.25 (d, 1H, J = 1.5 Hz), 7.22 (d, 1H, J = 1.5 Hz), 7.21 (d, 1H, J = 1.5 Hz), 7.20 (d, 1H, J = 1.5 Hz), 7.19 (s, 1H), 7.15 (s, 2H), 7.08 (s, 1H), 7.06 (s, 2H), 7.01 (d, 1H, J = 1.5 Hz), 7.00 (d, 1H, J = 1.5 Hz), 6.98 (s, 1H), 6.91 (d, 1H, J = 1.5 Hz), 6.88 (d, 2H, J = 1.5 Hz), 4.57 (q, 1H, J = 6.8 Hz), 4.46 (q, 1H, J = 6.8 Hz), 4.00 (s, 6H), 3.99 (s, 6H), 3.96 (s, 3H), 3.84 (s, 3H), 3.83 (s, 6H), 3.81 (s, 3H), 3.80 (s, 9H), 3.08−3.19 (m, 8H), 2.96−3.05 (m, 8H), 2.74 (d, 12H, J = 5.0 Hz), 2.32−2.39 (m, 4H), 2.14−2.23 (m, 4H), 1.70−1.87 (m, 2H), 1.61−1.68 (m, 2H), 1.52−1.59 (m, 2H), 1.41−1.50 (m, 4H). MALDI-TOF-MS calcd. for $C_{96}H_{124}N_{37}O_{18}$ (M + H): 2083.0. Found: 2083.1.

Im-Im-Py-(*R*)[Im-Im-Py-(*R*)$^{HNCO(CH_2)_4CO}$*γ*-Py-Py-Py-*β*-Dp]^{NH}*γ*-Im-Py-Py-*β*-Dp (4). This was obtained from Im-Im-Py-(*R*)$^{HNCO(CH_2)_4CO_2H}$*γ*-Py-Py-Py-*β*-Dp (**5L4**) as a white powder (1.2 mg, 28% isolated yield). UV (H_2O): λ_{max} 260 (56 000), 310 (104 280). ^{1}H NMR (DMSO-d_6): δ 10.29 (s, 2H), 10.28 (s, 1H), 10.11 (s, 1H), 10.05 (s, 1H), 9.92 (s, 1H), 9.89 (s, 1H), 9.88 (s, 1H), 9.71 (s, 2H), 9.20 (bs, 2H), 8.16 (d, 1H, J = 7.6 Hz), 8.11 (d, 1H, J = 7.6 Hz), 7.96−8.08 (m, 6H), 7.56 (s, 2H), 7.46 (s, 1H), 7.45 (s, 2H), 7.25 (d, 1H, J = 1.5 Hz), 7.22 (d, 1H, J = 1.5 Hz), 7.21 (d, 1H, J = 1.5 Hz), 7.20 (d, 1H, J = 1.5 Hz), 7.19 (s, 1H), 7.15 (s, 2H), 7.09 (s, 1H), 7.06 (s, 1H), 7.05 (d, 1H, J = 1.5 Hz), 6.99 (d, 1H, J = 1.5 Hz), 6.98 (s, 2H), 6.91 (d, 1H, J = 1.5 Hz), 6.88 (d, 2H, J = 1.5 Hz), 4.55 (q, 1H, J = 6.8 Hz), 4.44 (q, 1H, J = 6.8 Hz), 4.00 (s, 6H), 3.99 (s, 6H), 3.91 (s, 3H), 3.84 (s, 9H), 3.80 (s, 9H), 3.79 (s, 3H), 3.08−3.16 (m, 8H), 2.96−3.05 (m, 8H), 2.75 (d, 12H, J = 5.0 Hz), 2.32−2.39 (m, 4H), 2.14−2.24 (m, 4H), 1.70−1.83 (m, 2H), 1.61−1.67 (m, 2H), 1.41−1.59 (m, 8H). MALDI-TOF-MS calcd. for $C_{97}H_{126}N_{37}O_{18}$ (M + H): 2097.0. Found: 2097.2.

Construction of Plasmid DNA. Plasmids were constructed by inserting the following hybridized inserts into the *Bam*HI/*Hin*DIII polycloning site in pUC19. Plasmid **pPWLH1**: 5′-GATCCCGCGA-TGGCATACCATGCGCGCGCGCGCGATGGCATCCCATGCGCG-CGCGCGCGCGATGGGATCCCATGCGCGCGCGCGCGCGCGA-3′•5′-AGCTTCGCGCGCGCGCGCGCATGGGATCCCATCGCGCGC-GCGCGCGCATGGGATGCCATCGCGCGCGCGCGCGCATGGTATGCC-ATCGCGG-3′. The insert was obtained by annealing complementary synthetic oligonucleotides and was then ligated to the large *Bam*HI/*Hin*DIII restriction fragment of pUC19 using T4 DNA ligase. The ligated plasmid was then used to transform *E. coli* XL-1 Blue Supercompetent cells. Colonies were selected for α-complementation on 25 mL Luria-Bertani agarplates containing 50 mg/mL ampicillin and treated with XGAL and IPTG solutions and grown overnight at 37 °C. Well-defined white colonies were transferred into 100 mL Luria-Bertani medium containing 50 mg/mL ampicillin. Cells were harvested after overnight growth at 37 °C. Large-scale plasmid purification was performed using Qiagen purification kits. The presence of the desired insert was determined by dideoxy sequencing. DNA concentration was determined at 260 nm using the relation 1 OD unit = 50 mg/mL duplex DNA.

Preparation of 3′- and 5′-End-Labeled DNA Restriction Fragments. Plasmid pVRSS or pPWLH1 was simultaneously cut with *Eco*RI and *Pvu*II and then radiolabeled by 3′-fill in using [α-^{32}P-dATP], [α-^{32}P]-dTTP, and the Klenow fragment of DNA polymerase II at 37 °C for 25 min. The product mixture was purified on a 7% nondenaturing preparatory polyacrylamide gel (5% cross-link), and the desired fragment was isolated after visualization by autoradiography. The DNA was precipitated with 2-propanol (1.5 volumes). The pellet was washed with 75% ethanol, lyophilized to dryness, and then resuspended in 10 mL of RNase-free H_2O. For the 5′-labeling with pPWLH1, the two primer oligonucleotides, 5′-AATTCGAGCTCGGTACCCGG-3′ (forward) and 5′-CTGGCACGACAGGTTTCCCG-3′ (reverse), were constructed to complement the pUC19 *Eco*RI and *Pvu*II sites, respectively, such that amplification by PCR generates the 3′-filled *Eco*RI/*Pvu*II restriction fragment. The forward primer was radiolabeled using [γ-^{32}P]-dATP and polynucleotide kinase. The PCR product was purified on a 7% nondenaturing preparatory polyacrylamide gel (5% cross-link), visualized by autoradiography, and isolated as described above. Chemical sequencing reactions were performed according to published protocols.[12]

Quantitative DNase I Footprint Titrations, MPE Footprint Titrations, and Affinity Cleavage. All reactions were carried out in a volume of 400 μL according to the published procedures.[8] Quantitation by storage phosphor autoradiography and determination of equilibrium association constants were as previously described.[8]

Acknowledgment. We are grateful to the National Institutes of Health (GM-51747) for research support and the Swiss National Science Foundation for a postdoctoral fellowship to P.W. We thank G. M. Hathaway for the MALDI-TOF mass spectrometry, and J. A. Love for help with the 500 MHz NMR measurements.

Supporting Information Available: Synthetic details for the affinity cleavage conjugate, **2-EDTA**, and figures of quantitative DNase I footprinting experiments for results in Table 1 (PDF). This material is available free of charge via the Internet at http://pubs.acs.org.

JA020258K

(12) (a) Iverson, B. L.; Dervan, P. B. *Nucleic Acids Res.* **1987**, *15*, 7823. (b) Maxam, A. M.; Gilbert, W. S. *Methods Enzymol.* **1980**, *65*, 499.